Journal of Materials Chemistry A

Accepted Manuscript

This article can be cited before page numbers have been issued, to do this please use: N. Ma, C. Lin, N. Wu, Q. Liu, J. Ma, W. Meng, X. Wang, L. Zhang, X. Xu, Y. Zhao, L. Zhuang, J. Fan, J. Sun, R. Zhuo and X. Zhang, *J. Mater. Chem. A*, 2017, DOI: 10.1039/C7TA08002F.

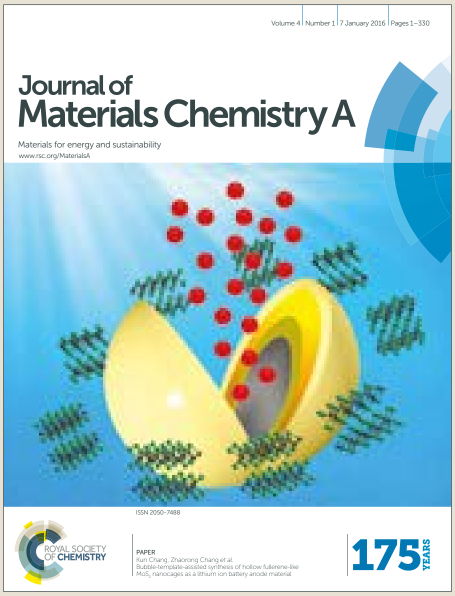

Volume 4 | Number 1 | 7 January 2016 | Pages 1–330

Journal of Materials Chemistry A

Materials for energy and sustainability

www.rsc.org/MaterialsA

ISSN 2050-7488

ROYAL SOCIETY OF CHEMISTRY

PAPER
Kun Chang, Zhaorong Chang et al.
Bubble-template-assisted synthesis of hollow fullerene-like MoS_2 nanocages as a lithium-ion battery anode material

175 YEARS

ROYAL SOCIETY OF CHEMISTRY

rsc.li/materials-a

View Article Online
DOI: 10.1039/C7TA08002F

Journal Name

COMMUNICATION

Stomata-like metal peptide coordination polymer

Ning Ma,[a†] Cong Lin,[b†] Nian Wu,[c] Qi Liu,[a] Jia-Le Ma,[d] Wei Meng,[e] Xiao-Shuang Wang,[a] Lu Zhang,[a] Xiaohui Xu,[a] Yifang Zhao,[b] Lin Zhuang,[c] Jun Fan,[d] Junliang Sun,[b]* Ren-Xi Zhuo,[a] and Xian-Zheng Zhang[a]*

Received 00th January 20xx,
Accepted 00th January 20xx

DOI: 10.1039/x0xx00000x

www.rsc.org/

The water-triggered reversible transformation plays a significant role in bio-systems. To develop artificial materials with reversible structural transformability under mild conditions would be helpful to understand how bio-systems work. Here we report on a flexible coordination polymer, Cu-(Gly-Thr)•2H_2O, whose structure can be controlled by humidity or temperature. This porous coordination polymer shows reversible single-crystal to single-crystal transformation with surprisingly high thermal stability. It was found that the ordered transformation occurs *via* coordination bonds breaking and reforming without changing coordination numbers and valence of the copper ion. This reversible transformation makes it especially efficient at taking up CO_2 under wet condition, which is similar to the function of plant stomata.

The stomata of leaves are specialized epidermal porous structures that balance the regulation of water vapour and CO_2 molecules exchange between environment and the plants.[1] The stomatal apparatus contains two guard cells that open and close depending on whether the plants need to hold on or lose water and CO_2. The guard cell signalling is functioned by the Stomagen (also called EPF-LIKE9) peptide.[2] Porous coordination polymers (PCPs) were reported to show similar structural transformation in response to specific stimuli, which provides a possibility for the design of stomata-like materials.[3,4] Soft PCPs are defined as porous crystals that possess both highly ordered networks and structural transformability.[4] Meanwhile, structural variations in soft PCPs can be approximately divided into two categories: those without any chain-scission degradation during adapting process and those that undergo guest molecules response with bond breaking and reforming reactions.[4-6] Most soft PCPs adopt the former type of transformation,[7] such as the 'breathing' guanidinium 1,2,4,5-tetra(4-sulfonatophenyl)-benzene (G_4TSPB),[8] two fold interpenetrating network $\{[Ni(bpe)_2(N(CN)_2)](N(CN)_2)(5H_2O)\}_n$[9] and side-chain controlled cooperative folding $Zn(GS)_2$ (GS = glycyl-serine),[10] *etc.*[11-13] However, the structural transformation with breaking and reforming of bonds in network linkage, is rarely reported,[6,14] especially at room temperature.[15]

Here we report on a flexible coordination polymer Cu-(Gly-Thr)•2H_2O (**1**), designated as WHU-3 (WHU stands for Wuhan University), which is built with Cu^{2+} and an dipeptide linker (Gly-Thr). The dipeptide is used to construct the coordination complex due to its good stability, flexibility, polydentate and biological activity.[2,16] The structural transformation (Fig. 1) was investigated by analyzing the change of chemical bonds and charge distribution. In addition, the CO_2 capture capability of the material was further studied in the absence or presence of water.

Water-triggered reversible transformation of the flexible coordination polymer. Crystals of **1** in the shape of monoclinic flakes (Fig. 2a) were obtained from the reaction of cupric

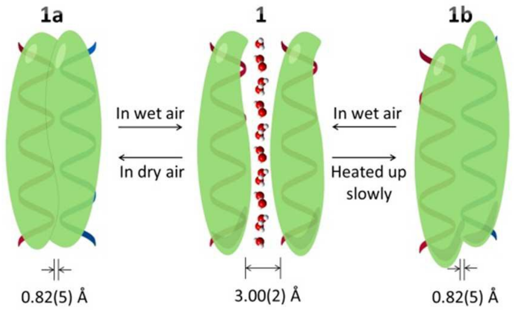

Fig. 1 Schematic diagram of structure transformation of Cu-(Gly-Thr)•2H_2O (**1**).

---

[a] Key Laboratory of Biomedical Polymers of Ministry of Education, The Institute for Advanced Studies & Department of Chemistry, Wuhan University, Wuhan 430072, P. R. China. E-mail: xz-zhang@whu.edu.cn

[b] College of Chemistry and Molecular Engineering, Peking University, Beijing 100871, P. R. China. E-mail: junliang.sun@pku.edu.cn

[c] Department of Chemistry, Hubei Key Lab of Electrochemical Power Sources, Wuhan University, Wuhan 430072, P. R. China,

[d] Department of Physics and Materials Science, City University of Hong Kong, Hong Kong SAR, P. R. China.

[e] Department of Materials Science and Engineering, College of Engineering, Peking University, Beijing 100871, P. R. China.

† N. M. and C. L. contributed equally.

Electronic Supplementary Information (ESI) available: [details of any supplementary information available should be included here]. See DOI: 10.1039/x0xx00000x

View Article Online
DOI: 10.1039/C7TA08002F

nitrate with Gly-Thr (GT) (Fig. S1) in water and methanol medium on a shaking table at 300 rpm for 20 minutes (see the Experimental Procedures in Supporting Information). The obtained complex (Fig. S2), is formed of a 1:1 motif of Cu^{2+} and GT^{2-} anion (Fig. S3). The Cu^{2+} is tetra-pyramidically coordinated to three GT ligands, and each ligand is coordinated to three Cu ions (Fig. 2b) by the C-terminal Gly carboxylate group, the N-terminal Thr amine group, and the nitrogen atom and oxygen atom of the peptide linkage (Fig. 2c). The intra-layer hydrogen bond between the -OH group from the Thr side chain and the terminal carboxylate group (O4H4A···O3, 2.037 Å) restricts the torsion of this flexible moiety, imposing the orientation of the water molecules and methyl groups (Fig. S4). Adjacent layers, with the same regular arranged layer structure, are bridged by hydrogen bonds through water molecules. The nitrogen atom of the terminal amino group forms hydrogen bonds with water guests (N1H1D···Ow1). And the close-connected H_2O (Hw3) is hydrogen-bonded with the oxygen (C2O1) from peptide in the next layer (Fig. 2e). Meanwhile, it is surprisingly that the inter-layer water molecules also form a stable layered hexagonal ice polymorph at room tempreture. As we will discuss later, the tetra-pyramidically coordinated Cu^{2+} ions and the hydrogen bonds contribute significantly to the structure transformation.

To investigate the water triggered structural change, *in situ* powder X-ray diffraction (PXRD) was performed by controlling the humidity. Single crystal X-ray diffraction of **1** and **1a** revealed that this structural change occurs *via* a single crystal-single crystal transformation (SCSCT), *i.e.*, from the afore mentioned $P2_1$ structure of **1** (a = 5.222 Å, b = 8.635 Å, c = 11.558 Å, β = 100.115°) to a new crystalline phase **1a** with a $P2_12_12_1$ symmetry (a = 5.287 Å, b = 8.718 Å, c = 17.773 Å). Compared with the structure of **1**, the dehydrated crystal **1a** shows a structural change, *i.e.*, although the two dimensional layer structure is retained, every second layer seems to be rotated 180 degrees along the c-axis during dehydration (Fig. 2e and 2f). In other words, the layers in **1** and **1a** stack in the AAAA and ABAB sequence, respectively (Fig. S6). However, the rotation of the whole layer requires to overcome a high reactive energy barrier.[17] It is speculated and proved later that the structural transformation occured with breaking and reforming of bonds. Moreover, **1a** switches the interlamellar spacing from 11.56 Å in **1** to 8.89 Å (the adjacent planes fit to the layers and the spacing taken as the distance between these planes). When the dehydrated single crystals of **1a** were exposed to the air with the relative humidity greater than 60% for more than 1 day, **1a** was able to return to the original monoclinic crystalline structure of **1**.

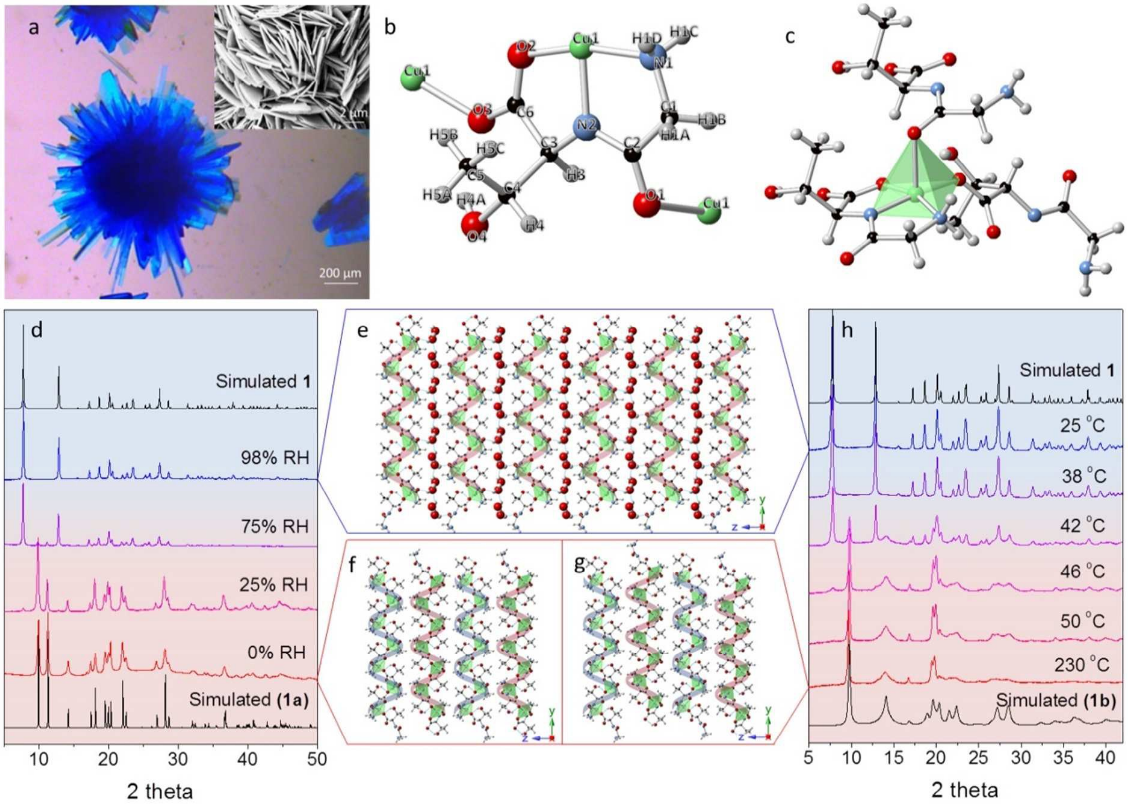

Fig. 2 Representation of the water-triggered metal peptide coordination polymer. a) Optical microscope and SEM image of the aggregated crystals of **1**. b) Colour map of the atom name. c) Coordination pattern of the tetra-pyramidically coordinated Cu ions of **1**, **1a** and **1b**. d) PXRD pattern in different humidity. The top and bottom ones are simulated PXRD patterns of **1** and **1a**, respectively. e) Crystal structure of **1**. f) Crystal structure of **1a**. g) Structural model of **1b**. h) *In situ* PXRD at mentioned temperature (°C) in air. (Cu, green; C, grey; N, blue; O, red; H, white)

View Article Online
DOI: 10.1039/C7TA08002F

Thus, the SCSCT is reversible, pointing an achievable pathway for egress and ingress of the water molecule without pressure-assistance, accompanied by a reversible 'Stomata-like breathing' of the crystal, in which the open and close of the 'guard' layers are controlled by the humidity. It is worth noting that the PXRD patterns of the sample in different humidity at room temperature confirmed the homogeneity of the structure transformation (Fig. 2d).

In situ variable temperature PXRD measurements (Fig. 2h) and thermogravimetric analysis were implemented to examine the thermal stability of this porous framework. A small change was observed at 42 ^{o}C with a series of new peaks detected and subsequently, the peaks of **1** gradually disappeared from 42 ^{o}C to 50 ^{o}C, indicating that the framework gradually changed. The stepwise thermogravimetric curve (Fig. S7) of **1** indicates that the release of the guest water molecules (measured loss 13.5 wt%, calculated 13.2 wt%), occurred at ~50 ^{o}C to give a new crystal form, which is stable up to ~235 ^{o}C. Therefore, the new crystal form (**1b**) (Fig. 2g) can be accomplished by slow heating up to the temperature range between 50 ^{o}C and 235 ^{o}C. On further heating, the peptide molecule is decomposed at the temperature about 237 ^{o}C, forming a brown amorphous phase. Mass spectrometric study (Fig. S8 and S9) indicated that methyl groups, ammonia, water, nitric oxide and carbon oxides were released at this point. No chemical decomposition was detected between the crystal transformation and ligand decomposition temperatures.

Based on the simulated PXRD (Fig. S11-13) by Diffax[17,18] and the *in situ* infrared spectra discussed later, it was suggested that during the transformation from **1** to **1b**, the intra-layer transformation occurred without very much inter-layer rearrangement. This result indicates that sluggish water evaporation upon heating can also change the intra-layer structure but retain stacking faults comparing with the structure of **1a**. Similar to the reversible phase transformation between **1** and **1a**, the reversible phenomenon was also detected in the case of **1b** when it was exposed to moisture, even after being heated up to 200 ^{o}C (Fig. S14), indicating an extraordinary stability of GT in this crystalline form. It is surprisingly for the peptide to be stable at such a high temperature since the bare peptide decomposes at 100 ^{o}C (Fig. S15-17).

Thus, the flexible porous compound **1** shows both reversible structural transformation between **1** and **1a** under different humidity at room temperature (reminiscent of the guard cells open the stomata under wet condition to abtain more CO_2 for photosynthesis) and between **1** and **1b** around the body temperature 38 ^{o}C (reminiscent of the guard cells close the stomata to hold on the water in the plants body at midday in the summertime) as shown in Fig. 1. Both transformations were triggered by the releasing and intercalation of water molecules and involved in the breaking and reforming of coordination bonds while the peptide molecules remained intact.

Experimental characterization and computational modelling of the structural transformation mechanism. To elucidate the possible mechanism of structural transformation from the wet state (**1**) to the dry state (**1a** or **1b**), the *in situ* variable temperature Fourier transform infrared (FT-IR) spectra of **1** were recorded as shown in Fig. 3a. No obvious shift was observed at 3445 cm^{-1} and 3306 cm^{-1}, which corresponds to a stretch asymmetric vibration $v_{as}(NH_2)$ and symmetric vibration $v_s(NH_2)$ of the terminal group on the dipeptide ligands, indicating that the NH_2 moieties remain coordinated during the dehydration process. Notably, the spectrum of **1** exhibited v(O-H) bands at 3275 cm^{-1}, and when the sample was heated to 72 ^{o}C, this peak shifted to 3365 cm^{-1}. In the meantime, peaks of C-H bonds from 3000 cm^{-1} to 2900 cm^{-1} shifted to lower frequency with the temperature increasing. These results indicated a decrease in the conjugation of the system of hydrogen bonded six-water member ring, which might be owing to a charge-transfer interaction between the lamellar structure and the water molecules.[7] This is consistent with our initial assumption that water molecules can induce changes in the coordination environments around the copper atoms, and the evacuation of water triggered the structural transition.

The carboxyl group of the dipeptide coordinated with Cu ions plays a key role for the transformation. The most characteristic peak, v_{as}(COO), is the asymmetric vibration of carboxyl groups around 1380 cm^{-1}, and its peak position indicates that carboxylate group COO^- is bridging two Cu ions. This peak shifts from 1385 cm^{-1} to 1378 cm^{-1}. More importantly, it became stronger from room temperature to 72 ^{o}C, and then turned weaker after further heating (Fig. 3a). The increasing of its intensity during the transformation indicates that the coordination mode of Cu-OCO-Cu has changed during the dehydration. The *in situ* FT-IR provided a possible mechanism, which is related to a bond breaking and reforming reaction occurred in a crystal by thermal induced desorption of water molecules.

The first-principles calculations were carried out to better understand the reaction pathway. According to charge density difference (CDD) schematic around Cu ions (Fig. 3b), each Cu^{2+} strongly binds with two N atoms and two O atoms. While, there are obvious increment of electron density in the middle region of Cu and the ligand atoms. Other than this, the depletion of electron density is near the ligand atoms.

View Article Online
DOI: 10.1039/C7TA08002F

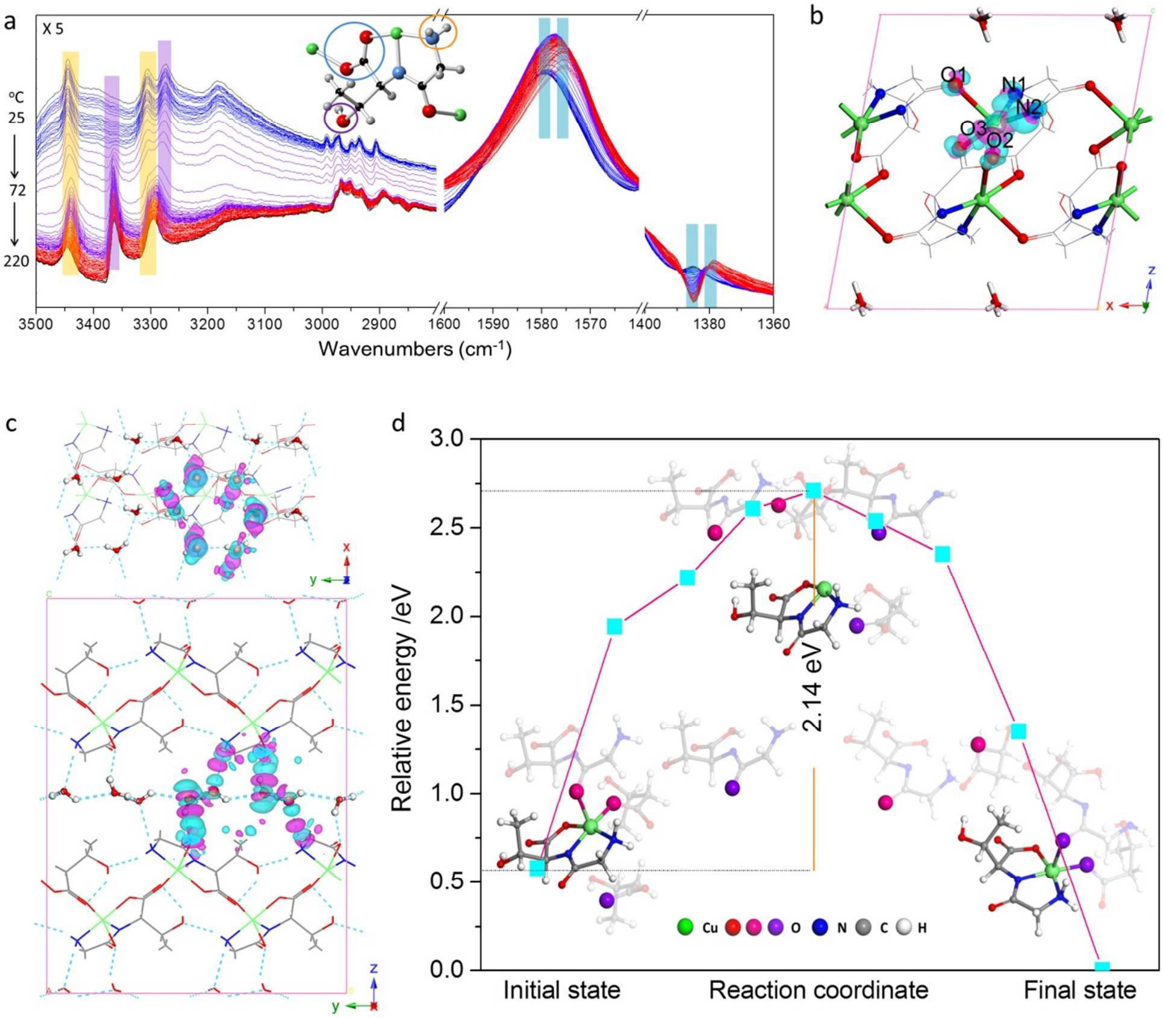

Fig. 3 Experimental characterization and computational modelling of the structural transformation. a) *In situ* FT-IR of **1** at varying temperatures under air, from blue to red represents temperatures from 25 °C to 220 °C. The initial and final curves were coloured black for clarity. b) The isosurface maps of charge density difference for Cu-(Gly-Thr)/H_2O system. c) The CDD isosurface maps for H_2O-Cu/(Gly-Thr) system. The CDD isovalues of Cu-(Gly-Thr)/H_2O system and H_2O-Cu/(Gly-Thr) system are 0.006 and 0.003 e/Å^3. The purple and cyan coloured isosurfaces correspond to negative and positive values, respectively. d) Relative energy of reaction pathway for transformation from wet to dry states.

According to the infrared spectra, the coordination mode of Cu-OCO-Cu has changed, while the Cu-N coordination remained during the phase transformation. Because O2, N1 and N2 are coordinated with the same Cu^{2+}, the chelation and sterically hindered effect restrict the movement of the peptide, which in turn influences the flexibility of Cu1-O2. While, there is no such bonding force or restriction for O1 and O3. Hence, it's reasonable to identify the breaking of Cu1-O3 during the transformation. Due to the far distance of Cu1 and O1 (Cu1···O1, 2.311 Å), there just exists depletion in the region near O1, and no accumulation in the middle region between Cu1-O1, demonstrating the relatively fragile electrostatic

View Article Online
DOI: 10.1039/C7TA08002F

interaction between them. It is also easy to identify the breaking of Cu1-O1 coordination bond. In fact, Cu^{2+} is penta-coordinated and due to the Jahn-Teller effect, Cu1-O1 is the weakest bond among them.[19,20] Therefore, we can make a reasonable assumption that the breaking of Cu1-O1 and Cu1-O3 bonds provides a possibility for one group attacking Cu^{2+} and another group leaving away.

To provide further insight into the effect of water molecules on the transformation, we calculated CDD for an isolated water (Fig. 3c), and it shows that hydrogen bond formation leads to intermolecular stabilization of water molecules. The hydrogen atom (Hw3) of water and the oxygen atom of peptide bond (C2O1) hold together by hydrogen bonds, while O1 is coordinated with the Cu cation. The increment of electron density around O1 is polarized by water, and the oxygen atom (Ow1) from water interacts with the nitrogen atom of terminal amino group (N1H1). These results suggest that intra-atomic electron configurations play a significant role in tipping the balance between water molecules and the frameworks, despite the larger changes in intermolecular energies.[21] In fact, these interactions may provide the internal driving force for the structural transformation.

According to the periodic electronic structure, a possible reaction pathway was animated to show the evolution of conformational state transition. Like domino effects, the constitutional units in the bulk phase are highly relevant during the transformation. The center copper cation and its related fragments before and after transformation were abstracted from primitive structures in wet and dry states as initial and final states, respectively (Fig. S20). Moreover, 9 frames on the trajectory from the initial state to the final state were generated *via* reaction preview in Material Studio (Movie S1 and S2). Then every single point energy was calculated (Fig. 3d). From the energy change as reaction coordinates, the difference of total energy between the peak point and initial state is 2.14 eV. This is a relatively low energy for the total system compared with those in the literature,[22] which confirmed the reasonability of the reversible transformation at ambient conditions. Note that many factors have been simplified in this calculation, for example, the remaining parts of peptides were not coordinated with copper, while they actually connected other coppers in the periodic system. Moreover, the hydrogen bonding interactions have not been considered between water layers and function groups of the ligands. These interactions responsibly contribute to the transformation mechanism and could possibly decrease the transformation energy significantly.

Water regulated CO_2 adsorption. To investigate the similarity of CO_2 adsorption behavior regulated by water between plant stomata and our material, we carried out dynamic adsorption experiments in the absence and presence of water. We firstly investigated the static adsorption behavior of the material at -78 °C (Fig. 4a). The amounts of adsorbed CO_2 for **1** and **1a** at the ordinary pressure are 45.90 cm^3/g and 7.65 cm^3/g, respectively, and the potential selective adsorption is very distinct. In addition, the tremendous hysteresis of water adsorption (Fig. S22) suggests a much stronger interaction between water and framework, which could be easily understood since the unusual flexibility of our PCPs is very closely related to water. The dynamic adsorption experiments were subsequently implemented in the absence (dry CO_2) and presence (wet CO_2) of water at 25 °C (Fig. 4b). For the dry CO_2, the breakthrough is rapid within only 19 s and the calculated adsorbed amount can be compared with the result from static adsorption, but the breakthrough in the presence of water is much slower with a 4 times longer breakthrough time. It is also apparent that the ascent rate of the wet state CO_2 after breakthrough is more sluggish. Such differences in breakthrough behavior are induced by the introducing of water.

To further explore the origin of the distinctive adsorption behavior, the materials after breakthrough experiments were identified by PXRD (Fig. S23). The material in the dry CO_2 is the dehydrated **1a** with a closed interlayer, making it hard for CO_2 to penetrate from the interlayer. While the relative humidity of the wet CO_2 is only 34% and could not induce the entire reformation of **1**. However, the fewer opened tunnels is propitious for CO_2 to travel through and interact with the pore walls, inducing a much larger adsorbed amount and longer

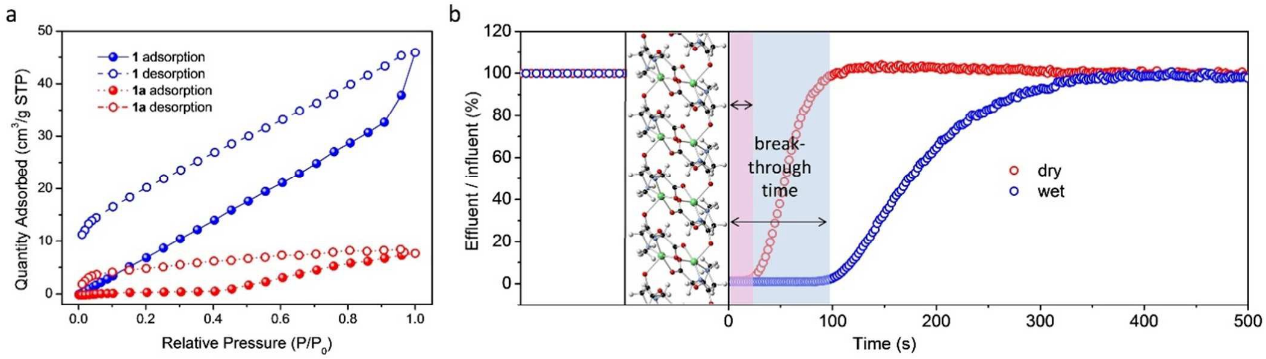

Fig. 4 Water regulated CO_2 adsorption behavior. a) CO_2 adsorption curves at -78 °C. b) Breakthrough cycle under dry and wet conditions at 25 °C. Breakthrough time is highlighted in pink and light blue.

View Article Online
DOI: 10.1039/C7TA08002F

breakthrough time. In the meantime, the small amount of water molecules also hinders the penetration of CO_2,[23] which contributes to the gentle ascent slope. We also believe that the water molecule is dynamically moving along with the gas flow, thus constantly opening and closing the interlayer. In conclusion, the CO_2 adsorption behavior of our PCPs material could be wisely regulated by water. It is very rare for PCPs exhibiting water enhanced CO_2 adsorption,[24-26] and to the best of knowledge, our PCPs material is the first one possessing such property through structure transformation.[27,28] The CO_2 adsorption behavior of our material is also very similar to that of botanical stomata, since guard cells would close stomata under very low ambient humidity thus preventing CO_2 taking up, and open stomata under wet ambience to take up CO_2 for photosynthesis.

Conclusions

In summary, a stomata-like metal peptide coordination polymer, Cu-(Gly-Thr)•$2H_2O$, was prepared with structural transformative ability, attributed to the charge-transfer interaction between the pore wall of the PCPs and the water molecules. It was found that a reversible SCSCT with bond breaking and reforming reactions occured without changing coordination numbers and valence of the copper ion. Adsorption experiments indicate our material possesses preferential water adsorption and enhanced CO_2 adsorption behavior regulated by water. We believe that these findings not only provide a better understanding of the intrinsic mechanism of the structural transformation, but also give hints for the structural evolution in bio-systems.

Acknowledgements

We acknowledge funding from the National Natural Science Foundation of China (51690152, 51233003 and 21471009). We thank Prof. Shaw Ling Hsu and Dr. Fang Chang Tsai for discussions; we thank the Department of Polymer Science and Engineering at University of Massachusetts (Amherst) for assistance with *in situ* FT-IR experiments and facilities. We thank Prof. Hexiang Deng for assistance with PXRD experiments and facilities.

Conflict of interest

There are no conflicts to declare.

Notes and references

1 H. Wang, N. Ngwenyama, Y. Liu, J. C. Walker, S. Zhang. *Plant Cell* 2007, **19**, 63-73.
2 J. S. Lee, M. Hnilova, M. Maes, Y.-C. L. Lin, A. Putarjunan, S.-K. Han, J. Avila, K. U. Torii. *Nature* 2015, **522**, 439-443.
3 S. Kitagawa, R. Kitaura, S. Noro. *Angew. Chem. Int. Ed.* 2004, **43**, 2334-2375.
4 H. Satoshi, S. Shimomura, S. Kitagawa. *Nat. Chem.* 2009, **1**, 695-704.
5 O. M. Yaghi, M. O'Keeffe, N. W. Ockwig, H. K. Chae, M. Eddaoudi, J. Kim. *Nature* 2003, **423**, 705-714.
6 B. Xiao, P. J. Byrne, P. S. Wheatley, D. S. Wragg, X. Zhao, A. J. Fletcher, K. M. Thomas, L. Peters, J. S. O. Evans, J. E. Warren, W. Zhou, R. E. Morris. *Nat. Chem.* 2009, **1**, 289-294.
7 C. Serre, C. Mellot-Draznieks, S. Surblé, N. Audebrand, Y. Filinchuk, G. Férey. *Science* 2007, **315**, 1828-1831.
8 W. C. Xiao, C. H. Hu, M. D. Ward. *J. Am. Chem. Soc.* 2014, **136**, 14200-14206.
9 T. K. Maji, R. Matsuda, S. Kitagawa. *Nat. Mater.* 2007, **6**, 142-148.
10 C. Martí-Gastaldo, D. Antypov, J. E. Warren, M. E. Briggs, P. A. Chater, P. V. Wiper, G. J. Miller, Y. Z. Khimyak, G. R. Darling, N. G. Berry, M. J. Rosseinsky. *Nat. Chem.* 2014, **6**, 343-351.
11 Y. J. Sheng, Q. B. Chen, J. Y. Yao, Y. X. Lu, H. L. Liu, S. Dai. *Angew. Chem. Int. Ed.* 2016, **55**, 3378-3381.
12 C. Serre, F. Millange, C. Thouvenot, M. Nogués, G. Marsolier, D. Louër, G. Férey. *J. Am. Chem. Soc.* 2002, **124**, 13519-13526.
13 J. A. Mason, J. Oktawiec, M. K. Taylor, M. R. Hudson, J. Rodriguez, J. E. Bachman, M. I. Gonzalez, A. Cervellino, A. Guagliardi, C. M. Brown, P. L. Llewellyn, N. Masciocchi, J. R. Long. *Nature* 2015, **527**, 357-361.
14 L. H. Cao, Y. S. Wei, S. Q. Zang, T. C. W. Mark. *Adv. Funct. Mater.* 2015, **25**, 6448-6457.
15 P. Mandal, M. J. Pitcher, J. Alaria, H. Niu, P. Borisov, P. Stamenov, J. B. Claridge, M. J. Rosseinsky. *Nature* 2015, **525**, 363-366.
16 Y. F. Wang, W. Qi, R. L. Huang, X. J. Yang, M. F. Wang, R. X. Su, Z. M. He. *J. Am. Chem. Soc.* 2015, **137**, 7869-7880.
17 A. Schneemann, V. Bon, I. Schwedler, I., Senkovsk, S. Kaskel, R. A. Fischer. *Chem. Soc. Rev.* 2014, **43**, 6062-6096.
18 M. P. Crosnier-Lopez, J. L. Fourquet. *Solid State Sci.* 2005, **7**, 530-538.
19 M. M. J. Treacy, J. M. Newsam, M. W. Deem. *Proc. R. Soc. London. A* 1991, **433**, 499-520.
20 L. L. Lohr. *Proc. Natl. Acad. Sci. U. S. A.* 1968, **59**, 720-725.
21 R. Janes, E. A. Moore. Metal-ligand bonding, The Open University, ISBN 0-85404-979-7, 2004, pp.23.
22 A. R. Dongré, J. L. Jones, Á. Somogyi, V. H. Wysocki. *J. Am. Chem. Soc.* 1996, **118**, 8365-8374.
23 A. M. Fracaroli, H. Furukawa, M. Suzuki, M. Dodd, S. Okajima, F. Gándara, J. A. Reimer, O. M. Yaghi. *J. Am. Chem. Soc.* 2014, **136**, 8863-8866.
24 S. Yang, J. Sun, A. J. Ramirez-Cuesta, S. K. Callear, W. I. F. David, D. P. Anderson, R. Newby, A. J. Blake, J. E. Parker, C. C. Tang, M. Schröder. *Nat. Chem.* 2012, **4**, 887-894.
25 E. S. Lenoir, C. Vagner, J. W. Yoon, P. Bazin, F. Ragon, Y. K. Hwang, C. Serre, J. S. Chang, P. L. Llewellyn. *J. Am. Chem. Soc.* 2012, **134**, 10174-10181.
26 A. Ö. Yazaydın, A. I. Benin, S. A. Faheem, P. Jakubczak, J. J. Low, R. R. Willis, R. Q. Snurr. *Chem. Mater.* 2009, **21**, 1425-1430.
27 A. Kumar, D. G. Madden, M. Lusi, K.-J. Chen, E. A. Daniels, T. Curtin, J. J. Perry IV, M. J. Zaworotko. *Angew. Chem. Int. Ed.* 2015, **54**, 14372-14377.
28 J. Liang, J. Su, X. Luo, Y. Wang, H. Zheng, H. Chen, X. Zou, J. Lin, J. Sun. *Angew. Chem. Int. Ed.* 2015, **127**, 7398-7402.

View Article Online
DOI: 10.1039/C7TA08002F

Figure for Table of Contents